Istituto Nazionale di Fisica Nucleare
Sottosezione di Bari

INFN/AE-70/8
29 Ottobre 1970

W. Delaney(*): THE SELF ENERGY OF THE ELECTRON AND THE MUON/ELECTRON MASS RATIO. -

ABSTRACT. -

A relationship between the masses of the electron propagating forward and backward in time is derived which suggests that the muon is the time reversed electron. This relationship is derived in a first approximation from the assumptions: 1) equality of the electron mass to its rest frame energy uncertainty, where this uncertainty is the inverse (units: h=c=1) of the uncertainty in the emission point of the self field (photons) retarded relative to the electron; 2) equality of the time forward electron mass to the electromagnetic mass of its combined retarded and advanced fields, which equality is formulated via the assumed equality of the electron momentum to the field momentum defined as the volume integral of the Poynting vector.
This derivation includes only mass contributions from the fields in the classical domain external to the field emission point uncertainty intervals. A more complete derivation is then given which depends upon 1) and 2) and: 3) the interpretation of the expression for the time forward electron mass obtained from 2) as integrals over the field emission times; 4) definition of electron space and time coordinates by spatially inverted (ingoing and outgoing, retarded, and advanced) fields where such definition may only be effected by fields propagating over space or time intervals exceeding the field emission point uncertainty intervals - so called external fields. With these considerations another, field point, uncertainty is also introduced. 5) Identification of the time forward electron time coordinate uncertainty interval relative to the time coordinates of its external fields and representation of the electron coordinate uncertainty by an assumed form for its fields in this time interval; this form is suggested by classical considerations. The final muon/electron mass ratio obtained is 206.7685.

(*) - Present Address: C. S. A. T. A., Istituto di Fisica, Bari, Italy.

In the limit of small electron velocity[1], $\vec{v}$, the momentum of the electromagnetic field of the electron, defined in terms of its electric, $\vec{E}$, and magnetic, $\vec{H}$, fields as

$$\vec{G} = \int d\Omega/4\pi \, dr \, r^2 \, \vec{E} \times \vec{H}$$

can be expressed in terms of the electron motion.

Using $\vec{H} = \vec{v} \times \vec{E}$ and the spherical symmetry of the $\vec{E}$ field[2]

$$\vec{G} = 2\,U/3\,\vec{v} \qquad \text{where} \qquad U = \int dr \, r^2 \, E^2$$

Identifying the field momentum with the electron momentum, the electromagnetic mass, $2U/3$, is assumed to be the experimental electron mass; thus

$$U = 3\,m/2$$

Assuming both retarded, $\vec{E}_1$, and advanced, $\vec{E}_2$, fields $\vec{E} = \vec{E}_1 + \vec{E}_2$ and $U = \sum_{i,j=1}^{2} U_{ij}$ where $U_{ij} = \int dr \, r^2 \, \vec{E}_i \cdot \vec{E}_j$. In particular $U_{ij} = \int_{\rho_i}^{\infty} dr \, r^2 \, E_i^2$ where ρ_i is a cutoff on the radial integration corresponding to the minimum limiting distance, for the field $\vec{E}_i$, at which classical electrodynamics breaks down and quantum considerations must be applied. If there were no cutoffs $\vec{E}_2(r) = -\vec{E}_1(r)$ for all r and $U = 0$. The cutoffs are interpreted as representing the field emission point uncertainties which can only be ignored at large distances (in the classical region). Since ρ_1 will turn out to be larger than ρ_2, U_{12} is cutoff at ρ_1 because it contains $\vec{E}_1$. With these cutoffs any contribution to the mass from the fields within the cutoff radii is ignored.

Calculating the fields as the negative gradients of the retarded, e/r, and advanced, $-e/r$, potentials

$$U_{11} = e^2/\rho_1 \qquad U_{22} = e^2/\rho_2 \qquad U_{12} = -e^2/\rho_1$$

Thus $$U = U_{11} + U_{22} + 2U_{12} = -e^2/\rho_1 + e^2/\rho_2 = 3m/2 \qquad \text{or}$$

(1) $$1/\rho_2 - 1/\rho_1 = 3m/2e^2$$

equation (1) may be written

(2a) $$1/T_2 + 1/T_1 = -3m/2e^2$$

where $T_1 = \rho_1$, $T_2 = -\rho_2$ are the photon retarded, advanced propagation

time uncertainties (the propagation times over the cutoff radii, in the rest frame).

The retarded propagation time uncertainty is equated to the inverse of the mass of the electron propagating forward in time (in the same direction as the retarded photons; $T_1 = 1/m$). Since the advanced photons would be retarded relative to a time reversed electron the magnitude of their propagation time uncertainty, ς_2, is equated to the inverse of the mass of the time reversed electron, $\varsigma_2 = -T_2 = 1/\mu$; this mass will be calculated.

From $1/T_1 = m$, $-1/T_2 = \mu$ equation (2a) may be written

(2b) $$\mu = 3m/2e^2 + m = 105.550 \text{ MeV}/c^2$$

where $1/e^2 = 137.03602$, $m = 0.5110041 \text{ MeV}/c^2$.

This value for μ suggests that the muon is the time reversed electron. This hypothesis has been advanced by Kaempffer[3] from general arguments based on symmetries of the solutions of the Dirac equation.

In the following an attempt is made to understand better the meaning of the cutoffs and to include effects from within the cutoffs in the mass calculation.

The fields $\vec{E}_1$, $\vec{E}_2$, expressed above as functions of the radial coordinate (field point) can be written for fixed field time as functions of the photon emission times. Likewise, the U_{ij} can be expressed as integrations over the emission time variables. The retarded, t_{01}, and advanced, t_{02}, emission times are related to the field space, r, and time, t, coordinates by

(3) $$r = t - t_{01} = t_{02} - t$$

(t_{01} and t_{02} are the emission times of retarded and advanced photons with common r at time t).
It is essential to recognize that all coordinates and intervals refer to the electron rest frame where the electron is at the origin of spatial coordinates.

Thus for[1]

(4a) $$t_{01} < t - \varsigma_1, \qquad \vec{E}_1 = e\vec{n}/(t - t_{01})^2$$

and for

(4b) $$t_{02} > t + \varsigma_2, \qquad \vec{E}_2 = -e\vec{n}/(t_{02} - t)^2$$

$$(4c) \qquad U_{11} = \int_{-\infty}^{t-\rho_1} dt_{01}\,(t-t_{01})^2\, e^2/(t-t_{01})^4$$

$$(4d) \qquad U_{22} = \int_{t+\rho_2}^{\infty} dt_{02}\,(t_{02}-t)^2\, e^2/(t_{02}-t)^4$$

$$(4e) \qquad U_{12} = \int_{-\infty}^{t-\rho_1} dt_{01}\,(t-t_{01})^2\, e/(t-t_{01})^2(-e)/(t_{02}-t)^2$$

Using (3) U_{12} may be expressed entirely in terms of the integration variable t_{01}.

$$U_{12} = \int_{-\infty}^{t-\rho_1} dt_{01}\,(t-t_{01})^2\, e/(t-t_{01})^2(-e)/(t-t_{01})^2$$

In U_{12} the advanced field from t_{02} combines with the retarded field from t_{01} at their common space-time point.

The U_{ij} expressed in this form are interpreted as the contributions to the mass of an electron when it has the (arbitrary but fixed) time coordinate t and is propagating forward in time. In equations (4a-e) the only electron (field emission) time coordinates considered are those relevant to retarded (advanced) fields propagating to t over a time interval $\geq \rho_1$ ($\geq \rho_2$). This is analogous to the classical situation where the field in the region external to a spherically symmetric charge distribution can be calculated as if the source were a point at the radial coordinate origin; here the fields in the region external to the source uncertainty (hereafter called external fields) are calculated as if the source space time coordinates were precisely specified. It is suggested that these external fields may be used to define the essentially classical quantities of spatial and temporal intervals and coordinates and that only by means of such fields can such quantities be inferred to have physical significance. The source radial coordinate is identified as the space point to which an ingoing retarded (advanced) field would converge from the surface (sphere) upon which the outgoing retarded (advanced) field from the source assumes a constant value. These ingoing fields propagate from the outgoing field space-time field points to the source space point over time intervals equal to the propagation time of the outgoing fields from their source space coordinate to their field space-time points; the possibility of such ingoing fields propagating over such time intervals is inferred from the existance of the outgoing fields propagating over these time intervals. The radius of the sphere within the surface of constant field intensity in a reference system at its origin can be defined as half the sum of the field propagation time from emission time at the origin to the surface at the field time plus the propagation time of a field from this field time back inward to the origin. These ideas apply only in the classical region were the spherical surface of constant field intensity has a re-

lationship to unique spatial and temporal intervals.

The hypothesis of the existence of both retarded and advanced fields states that if the emission time of the outgoing field is a retarded (advanced) emission time then the arrival time of the ingoing field at the origin is an advanced (retarded) emission time.

Within this classical framework it is desired to define the time coordinate of the electron propagating forward in time at which its mass is being calculated. For this purpose four time coordinates are considered: the advanced field emission, t_{02}, and field, t_2, times and the retarded field emission, t_{01}, and field, t_1, times where $t_{02} > t_2 > t_1 > t_{01}$.

Thus $t_{02} = t_2 + \epsilon_2, \quad t_1 = t_{01} + \epsilon_1, \quad t_2 = t_1 + \epsilon_3, \quad \epsilon_1, \epsilon_2, \epsilon_3 > 0$

The electron time coordinate is defined to be between t_{01} and t_{02} in the limit that t_{02} approaches t_2, t_{01} approaches t_1, and t_2 approaches t_1 where these limits are constrained by the requirement that they be definable in terms of propagations of external fields.

The retarded field emission time uncertainty, ρ_1, limits the approach of t_{01} to t_1, the minimum limiting value of ϵ_1 is $\epsilon_1 = \rho_1$, ρ_1 is equated to the inverse of the mass of the forward electron.

Likewise the advanced field emission time uncertainty, ρ_2, limits the approach of t_{02} to t_2, the minimum limiting value of ϵ_2 is $\epsilon_2 = \rho_2$. Since the advanced field would be retarded relative to a time reversed electron ρ_2 is equated to the inverse of the mass of the time reversed electron.

No electron time coordinates have as yet been defined in terms of external fields in the interval between t_{01} and t_{02}. The limiting value of ϵ_3 is chosen so that this may be done. Equation (3) expresses the relationship between the retarded, t_{01}, and advanced, t_{02}, emission times at given r and t; t_{01} (t_{02}) is obtained by reflection of t_{02} (t_{01}) in t. This reflection rule restates the relationship of the radial field coordinate to the outgoing and ingoing field propagation time intervals which define it and the relationship of the field time coordinate to emission time coordinates of retarded and advanced fields symmetrically located on the time axis relative to it. Using this idea the minimum limiting value of ϵ_3 is equated to ρ_2 since in this way all electron emission time coordinates are defined in the interval from $t_1 - \rho_1$ to t_1 by reflection of advanced external field emission times in t_2. This may be seen by writing (3) as

(5) $$r_2 = t_{02} - t_2 = t_2 - t_{01} = (t_1 - t_{01}) + \rho_2 = r_1 + \rho_2$$

for $t_{02} = t_2 + \rho_2, \quad t_{01} = t_1$; for $t_{02} = t_2 + \rho_2 + \rho_1, \quad t_{01} = t_1 - \rho_1$

The result of equations (2a-b) indicate $\delta_1 > 2\,\delta_2$ in which case it is not possible to define advanced field emission times in the interval between t_2 and $t_2 + \delta_2$ by reflection of retarded external field emission times. Thus electron time coordinates are not defined between t_1 and $t_2 + \delta_2$, but since they are defined between $t_1 - \delta_1$ and t_1 the electron may be taken to be in this interval when the previously indicated limits are taken. The significance of the limit $\epsilon_3 = \delta_2$ is emphasized by the consideration that if ϵ_3 were less than δ_2 electron time coordinates could only be defined in part of the interval from $t_1 - \delta_1$ to t_1; the electron time coordinate would have to be taken to be uncertain within an interval less than $\delta_1 = 1/m$ at variance with the uncertainty relation.

These conclusions about the electron-field system have implications relevant to the expression for the electron mass. Rewriting (4a-e) with the retarded t_1, and advanced, t_2, field times distinguished:

(6a) for $t_{01} < t_1 - \delta_1$ $\quad \vec{E}_1 = e\vec{n}/(t_1 - t_{01})^2$

(6b) for $t_{02} > t_2 + \delta_2$ $\quad \vec{E}_2 = -e\vec{n}/(t_{02} - t_2)^2$

$$(6c) \qquad U_{11} = \int_{-\infty}^{t_1 - \delta_1} dt_{01}(t_1 - t_{01})^2\, e^2/(t_1 - t_{01})^4 = e^2/\delta_1$$

$$(6d) \qquad U_{22} = \int_{t_2 + \delta_2}^{\infty} dt_{02}(t_{02} - t_2)^2\, e^2/(t_{02} - t_2)^4 = e^2/\delta_2$$

$$(6e) \qquad U_{12} = \int_{-\infty}^{t_1 - \delta_1} dt_{01}(t_1 - t_{01})^2\, e/(t_1 - t_{01})^2 (-e)/(t_{02} - t_2)^2$$

From the discussion preceeding, these equations give the contributions to the forward electron mass when its retarded photons have time coordinate t_1, its advanced photons have time coordinate t_2 and the electron itself has a time coordinate uncertain between t_1 and $t_1 - \delta_1$.

If there were only one field it would be intuitively suggestive to define the present time to which the mass calculation refers as the field time; with the two fields separated by the time interval $t_2 - t_1 = \delta_2$ the present time would be uncertain by δ_2. This uncertainty is of a peculiar type however, $t_1(t_2)$ is the present time as approached from the past (future); time coordinates between t_1 and t_2 have no obvious physical interpretation. This gives rise to the difficulty of considering two present times, one in the space-time of the retarded photons, another in the space-time of the advanced photons. Although intuitively difficult such language is convenient and will be used; below an interpretation of this field (present) time uncertainty will be suggested in which it will assume a more familiar aspect.

Using (5) it was seen that reflection of an advanced emission time, t_{02}, in the field time t_2 could define a retarded emission time t_{01}. In general (5) means that when the implied retarded emission time, t_{01}, is used with the retarded field time, t_1, an apparent space coordinate, r_1, of the advanced photon at the present time in the space of retarded photons is obtained. The minimum value of r_2, ρ_2, corresponds to $r_1 = 0$, or $t_{01} = t_1$ (the undefined times between t_1 and $t_2 + \rho_2$ would correspond to negative r_1). Using (5), (6d) may be written

$$U_{22} = \int_{-\infty}^{t_1} dt_{01}\,(t_1 - t_{01} + \rho_2)^2\, e^2/(t_1 - t_{01} + \rho_2)^4 =$$

$$= \int_0^{\infty} dr_1\,(r_1 + \rho_2)^2\, e^2/(r_1 + \rho_2)^4$$

The integral over t_{02}, cut off at $t_2 + \rho_2$, may be expressed as an integral over all the space or time of the retarded photons, and is the complete contribution to the electron mass from photons emitted after t_1 (no contribution from the undefined times between t_1 and $t_2 + \rho_2$).

It is also possible to consider, for retarded emission times $t_{01}(t_{01} < t_1 - \rho_1)$, the definition of advanced emission times, t_{02}, by reflection of t_{01} in t_1. Thus (3) becomes:

$$r_1 = t_1 - t_{01} = t_{02} - t_1 = (t_{02} - t_2) + \rho_2 = r_2 + \rho_2 \tag{7}$$

In (7) r_2 is the apparent space coordinate of the retarded photon from t_{01} at the present time in the space of advanced photons. In U_{12}, $\vec{E}_2$ is evaluated at this point; thus, expressing U_{12} entirely in terms of the integration variable t_{01}:

$$U_{12} = \int_{-\infty}^{t_1 - \rho_1} dt_{01}\,(t_1 - t_{01})^2\, e/(t_1 - t_{01})^2\,(-e)/(t_1 - t_{01} - \rho_2)^2 =$$

$$= \int_{\rho_1}^{\infty} dr_1\, r_1^2\, e/r_1^2\,(-e)/(r_1 - \rho_2)^2 = \tag{8}$$

$$= -e^2/(\rho_1 - \rho_2) \simeq -e^2/\rho_1 - e^2\rho_2/\rho_1^2$$

In order to extend the integration in the U_{11} and U_{12} terms to $t_{01} = t_1$ (or, from $r_1 = 0$) the electron coordinate uncertainty is represented in terms of the $\vec{E}_1$ field by defining $\vec{E}_1$ as the field of a uniform spherical charge distribution of radius ρ_1 and total charge e .

(9) Thus for $t_1 - \rho_1 < t_{01} < t_1 \quad (r_1 < \rho_1) \qquad \vec{E}_1 = e\vec{n} r_1/\rho_1^3$

Above electron time coordinates were defined for times between t_1 and $t_1 - \rho_1$, but the electron present time coordinate is uncertain in this interval. This implies that although time coordinates in this interval exist as possible electron time coordinates, the order in which the electron assumes the time coordinates cannot be specified. If a photon propagation is considered between two possible electron time coordinates either may be considered the emission, and the other the field, time. Also the emission time associated with any time coordinate considered as a field time may be before or after the field time. These arguments imply both retarded and advanced field emission in this time interval in such a symmetric way that the (expected classical) relation $\vec{E}_2 = -\vec{E}_1$ is suggested. Thus, when the range of integration in U_{12} is extended to $r_1 = 0$ the $\vec{E}_2$ field is also defined by a term like (9) but its form is slightly different due to the requirement that the $\vec{E}_2$ field in U_{12} be continuous at $r_1 = \rho_1$.

Thus for $t_1 - \rho_1 < t_{01} < t_1 \quad (r_1 < \rho_1) \qquad \vec{E}_2 = -e\vec{n}(r_1 + 2\rho_2)/\rho_1^3$

Evaluating the contribution to the mass from $r_1 < \rho_1$ from extending the U_{12} integration to $r_1 = 0$,

$$(10) \qquad U'_{11} = \int_0^{\rho_1} dr_1 \, r_1^2 \, e^2 \, r_1^2/\rho_1^6 = e^2/5\rho_1$$

Evaluating the contribution to the mass from $r_1 < \rho_1$ from extending the U_{12} integration to $r_1 = 0$

$$(11) \qquad U'_{12} = -\int_0^{\rho_1} dr_1 \, r_1^2 \, e^2 \, r_1 (r_1 + 2\rho_2)/\rho_1^6 = -e^2/5\rho_1 - e^2\rho_2/2\rho_1^2$$

Combining all the contributions to the electron mass (6c), (6d), (8), (10), (11)

$$U = U_{11} + U_{22} + 2U_{12} + U'_{11} + 2U'_{12} =$$

$$= e^2/\rho_1 + e^2/\rho_2 - 2e^2/\rho_1 - 2e^2\rho_2/\rho_1^2 + e^2/5\rho_1 - 2e^2/5\rho_1 - e^2\rho_2/\rho_1^2 = 3m/2$$

Thus with $\rho_1 = 1/m, \qquad \rho_2 = 1/\mu$

$$\mu = 3m/2e^2 + 6m/5 + 3m^2/\mu$$

$$\mu/m = 3/2e^2 + 6/5 + 3m/\mu$$

Defining $$a = 3/2e^2 + 6/5$$

(12) $$\mu/m = (a + (a^2 + 12)^{1/2})/2 \simeq a + 3/a$$

(the negative root is disregarded since the masses are assumed positive). Evaluating (12) with the above quoted value for e^2

$$\mu/m = 206.7685$$

Experimentally the muon/electron mass ratio is[4] 206.769 ± 0.003.

In order to give a more intuitively appealing interpretation of the field (present) time uncertainty an idealized field measurement situation is suggested. The problem here is to measure the field with minimal uncertainty, where this uncertainty is directly related to the uncertainty in the specification of the time at which the field is absorbed; above this field time uncertainty was found to be δ_2.

It is assumed that the absorption of a retarded (advanced) field is equivalent to the emission of an advanced (retarded) field. In order to realize the minimal field time uncertainty the retarded (advanced) field is measured with time forward (backward) electrons. The retarded field absorption, being equivalent to an advanced field emission, introduces an uncertainty in the field time of δ_2. Since the advanced field is retarded relative to a time reversed electron its absorption by such an electron is equivalent to the emission of a field advanced with respect to this electron, again a field time uncertainty of magnitude δ_2 is introduced.

A significant aspect of this picture is the possibility of giving meaning to the time coordinates between the previously defined retarded, t_1, and advanced, t_2, field times associated with an electron by means of other objects which measure these fields.

It would also seem significant that the minimization of the field uncertainty is achieved by measuring the fields with electrons propagating in the same time direction as the fields in accordance with the concept of a time ordered causality in the interaction between different objects.

ACKNOWLEDGMENT. -

The author would like to thank Professor Luciano Guerriero for many valuable discussions.

10.

REFERENCES AND FOOTNOTES. -

(1) - Units and symbols: $\hbar = c = 1$, $\vec{E}, \vec{H}$ fields are in Gaussian units $d\Omega =$ = unit solid angle, r = radial distance $r = |\vec{r}|$, $\vec{n}$ is unit 3 vector = $\vec{r}/r$.
(2) - W. K. H. Panofsky and M. Phillips, Classical Electricity and Magnetism (Addison Wesley, 1956) Ch. 21, p. 385.
(3) - F. A. Kaempffer, Concepts in Quantum Mechanics (Academic Press, 1965, Sect. 17, 19.
(4) - B. N. Taylor, W. H. Parker and D. N. Langenberg, The Fundamental Constants and Quantum Electrodynamics (Academic Press, 1969).

Istituto Nazionale di Fisica Nucleare
Sezione di Bologna

INFN/AE-70/9
28 Dicembre 1970

SYSTEMATIC SEARCH FOR EXOTIC RESONANCES IN K^-d INTERACTIONS AT 3 GeV/c.

S. A. B. R. E. Collaboration:

G. Giacomelli, P. Lugaresi-Serra, A. Minguzzi-Ranzi, A. M. Rossi
Istituto di Fisica and Istituto Nazionale di Fisica Nucleare, Bologna;

R. Barloutaud, J. C. Scheuer
Dèpartment de Physique de Particules Elementaires, Centre d'Etudes Nucleaires, Saclay;

A. M. Bakker, W. Hoogland, J. C. Kluyver
Zeeman Laboratorium, Amsterdam(x);

G. Alexander(o), Y. Eisenberg
The Weizmann Institute, Nuclear Physics Department, Rehovoth;

J. Goldberg(+), A. Rougé
Ecole Polytechnique, Paris.

ABSTRACT. -

A systematic search for exotic states produced in K^-d interactions at 3 GeV/c is reported. From the analysis of the mass spectra of strange mesons, non-strange mesons, hyperons with $S = -1$ and $S = -2$ upper limits for the production cross sections of exotic resonances may be placed at one or two orders of magnitude smaller than for the production of normal resonances of same strangeness and baryon number.

(x) - The work in Amsterdam is part of the joint research programs of FOM and ZWO.
(o) - Present address: Tel-Aviv University, Tel-Aviv.
(+) - Present address: Technion, Haifa.

1. - INTRODUCTION. -

In this report we shall discuss in detail the results of a systematic bubble chamber search for exotic resonances produced in K^-d interactions at 3 GeV/c[1].

We shall be concerned with states which are exotic as far as isotopic spin, and therefore cannot be placed in the lowest SU(3) representations. In fact we search only for negatively doubly charged states.

The experimental situation on exotic resonances is not yet conclusive[1-3], though several indications for their existence have been reported in a number of formation[4-7] and production[8-12] experiments as well as in phase shift analyses[13] and by indirect methods[14-16].

In K^-n interactions many exotic states are easily accessible; a large fraction of these states may be produced in quasi-two-body reactions, in configurations where exchanges in the t- or u-channels of non-exotic systems are allowed. The analysis of the exotic states produced in quasi-two-body reactions has been the subject of a separate publication[1]. Here we shall show the histograms for exotic mass combinations for each quasi-two-body reaction as well as for more complicated final states.

Some structures, at the 2-5 standard deviation level, are observed in several mass distributions. Their statistical significance is too limited and moreover most of them do not coincide in the mass spectra of various final states.

2. - EXPERIMENTAL. -

The 81 cm Saclay bubble chamber filled with deuterium was exposed to a 3 GeV/c, electrostatically separated, K^- beam at the CERN protonsynchrotron. 650.000 pictures were taken and scanned twice. The events were measured with conventional projectors and analyzed with the CERN chain of computer programs. Details of the experimental methods, in particular for eliminating ambiguities and computing cross sections, can be found in ref. (17). The experiment corresponds to 6.8 events/μb/nucleon.

In this paper we shall consider the following final states (the spectator proton, defined as that proton with a laboratory momentum smaller than 300 MeV/c, is neglected):

(1) $pK^-\pi^-$, $pK^-\pi^-\pi^o$, $pK^-\pi^-MM$

(2) $\pi^+K^-\pi^-n$, $\pi^+K^-\pi^-MM$

(3) $p\pi^-\pi^-\bar{K}^o$, $p\pi^-\pi^-\bar{K}^o\pi^o$, $p\pi^-\pi^-\bar{K}^o MM$

(4) $\pi^+\pi^-\pi^-\bar{K}^o n$, $\pi^+\pi^-\pi^-\bar{K}^o MM$

(5) $\pi^+\pi^-\pi^-\Lambda^o(\Sigma^o)$, $\pi^+\pi^-\pi^-\Lambda^o\pi^o$, $\pi^+\pi^-\pi^-\Lambda^o MM$

(6) $\pi^+\Sigma^-\pi^-$, $\pi^+\Sigma^-\pi^-\pi^o$, $\pi^+\Sigma^-\pi^- MM$

(7) $\Sigma^+\pi^-\pi^-$, $\Sigma^+\pi^-\pi^-\pi^o$, $\Sigma^+\pi^-\pi^- MM$

(8) $K^+\Xi^-\pi^-$, $K^+\Xi^-\pi^-\pi^o$, $K^+\Xi^-\pi^- MM$

where MM = missing mass means that more than one neutral unobserved particle is present in the final state. These reactions allow the study of exotic resonances in the following mass combinations:

(9) strange mesons $K^-\pi^-$, $(\bar{K}\pi\pi)^{--}$, $(\bar{K}\pi MM)^{--}$

(10) non strange mesons $\pi^-\pi^-$, $\pi^-\pi^-\pi^o$

(11) baryons with S = 0 $n\pi^-\pi^-$

(12) baryons with S = -1 $\Lambda^o\pi^-\pi^-$, $\Sigma^-\pi^-$, $(\Sigma\pi\pi)^{--}$

(13) baryons with S = -2 $\Xi^-\pi^-$.

Figures 1-14 show the effective mass distributions for the combinations (9)-(13). Some graphs include two hystograms, the first with the total number of events available for that reaction channel and the other one corresponding to a relevant subset of the data, with the selections explained in the figure captions. The experimental distributions are compared with the predictions of normalized relativistic phase space, shown on the graphs by solid lines. Phase space was computed by means of a Montecarlo program which takes into account the motion of the target neutron, according to the Hulthen wave function, and the reflections from dominant resonances. We may estimate an approximate 3-standard deviation upper limit for the production of an exotic resonance of a certain mass and width Γ ($\Gamma \approx 100$ MeV) using the formula:

(14) $$\Delta \lesssim (N - N') + 3\sqrt{N}$$

where N and N' represent the number of measured events and the number of phase space events inside one width Γ.

3. - STRANGE MESONS. -

The exotic strange mesons accessible in this experiment have $I_z = \pm 3/2$; they are the $K^-\pi^-$, $\bar{K}^o\pi^+$ and $(\bar{K}\pi\pi)^{--}$ states. The three-body $\bar{K}\pi\pi$ states may be observed as $K^-\pi^-\pi^o$, $\bar{K}^o\pi^-\pi^-$ and as $K^{*-}(890)\pi^-$.

3.1. - $K^-\pi^-$ and $\bar{K}^o\pi^+$ states.

Figure 1 shows the $K^-\pi^-$ effective mass distributions for three reactions.

The $pK^-\pi^-$ final state is particularly suitable for a search of possible $K^-\pi^-$ resonances because of the relatively small percentage of normal resonance production and because of the large number of events available for the analysis. The events come from the "three-prong" and "four-prong with spectator proton" topologies. The $K^-\pi^-$ effective mass distribution shown in Fig. 1a is compared with the prediction of phase space, taking into account the reflections of $\Lambda(1520)$ and $\Lambda(1815)$. The subset of Fig. 1a contains those events for which the square of the four momentum transferred to the $K^-\pi^-$ complex is smaller than $0.5\ (GeV/c)^2$; in this case the reaction mechanism should be dominated by one-pion-exchange[18].

The $pK^-\pi^-\pi^o$ and $pK^-\pi^-MM$ final states come from events of the same topology as for the $pK^-\pi^-$ final state. However, whilst the $pK^-\pi^-$ reaction is kinematically four times over-constrained, the $pK^-\pi^-\pi^o$ is only once over-constrained, and the $pK^-\pi^-MM$ is not constrained at all. This means that the percentage of ambiguous events becomes larger and that the experimental resolutions become broader, particularly for those distributions involving the neutral particles. Fig. 1b shows the $K^-\pi^-$ effective mass for the $pK^-\pi^-\pi^o$ final state.

The other final state $\pi^+K^-\pi^-n$ analysed for the $K^-\pi^-$ combination comes again from events of the "three-prong" and "four-prong" topologies. In this reaction there is a rather large production of resonances, particularly of the $K^{*o}(890)$ and of the $\Delta^-(1236)$. Therefore it may be more difficult to detect the presence of possible $K^-\pi^-$ states. Fig. 1c shows the $K^-\pi^-$ effective mass distribution for all the $\pi^+K^-\pi^-n$ events as well as for the subset for which the $K^{*o}(890)$ and $\Delta^-(1236)$ were removed.

Figure 2 shows the $\bar{K}^o\pi^+$ effective mass distribution for the final state $\pi^+\pi^-\pi^-\bar{K}^on$. The number of events available for this reaction is rather limited. The events belong to the topologies "three-prongs plus V^o" or "four-sprongs with spectator proton plus V^o". The $K^-\pi^-$ and $\bar{K}^o\pi^+$ mass distributions do not give any indication for a significant enhancement.

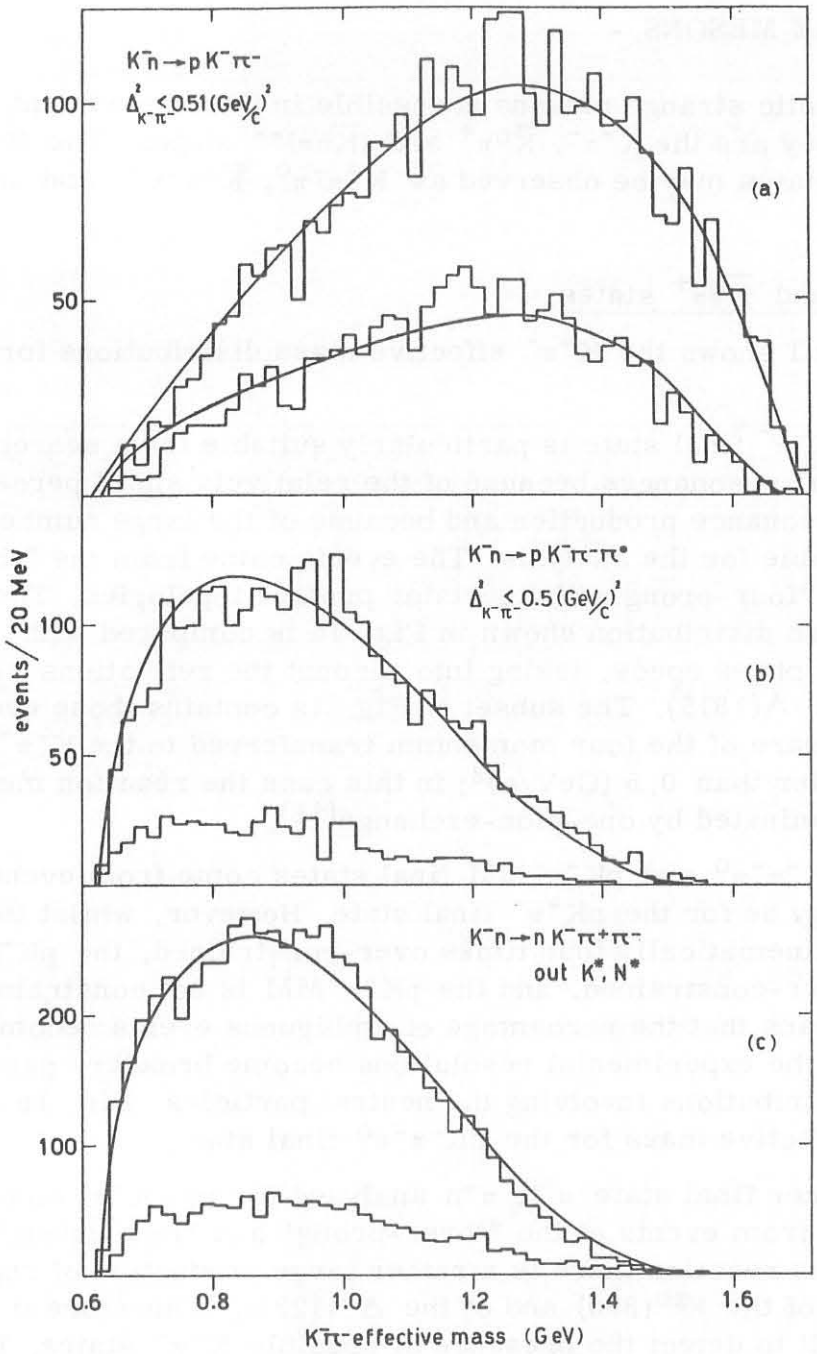

FIG. 1 - $K^-\pi^-$ effective mass distributions in the :

a) $pK^-\pi^-$ final state. The subset corresponds to events for which $\Delta^2_{K^-\pi^-} < 0.5\ (GeV/c)^2$. The solid lines represent the phase space predictions normalised to the total number of events. Reflections from the production of dominant resonances have been taken into account.

b) $pK^-\pi^-\pi^o$ final state. Also shown are the events with $\Delta^2_{K^-\pi^-} < 0.5\ (GeV/c)^2$.

c) $K^-\pi^+\pi^-n$ final state. The subset corresponds to removing $K^{*o}(890)$ and $\Delta^-(1236)$.

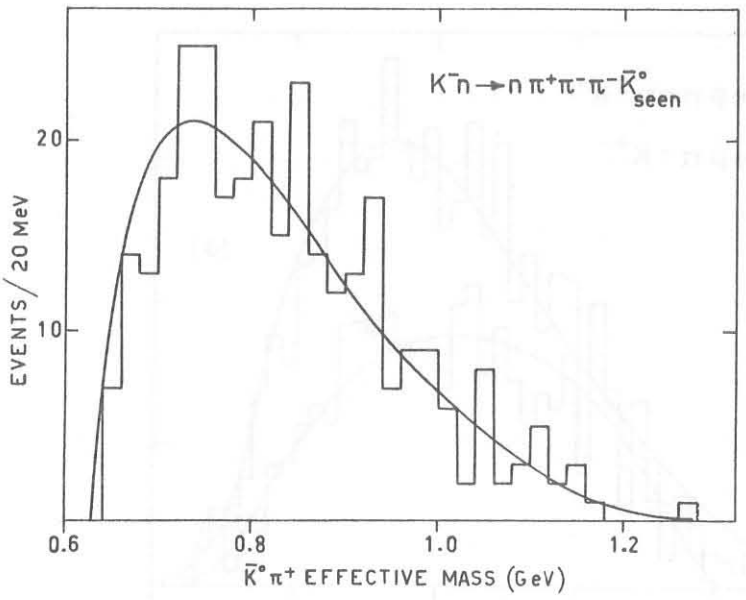

FIG. 2 - $\bar{K}^0\pi^+$ effective mass distribution in the $\pi^+\pi^-\bar{K}^0 n$ final state.

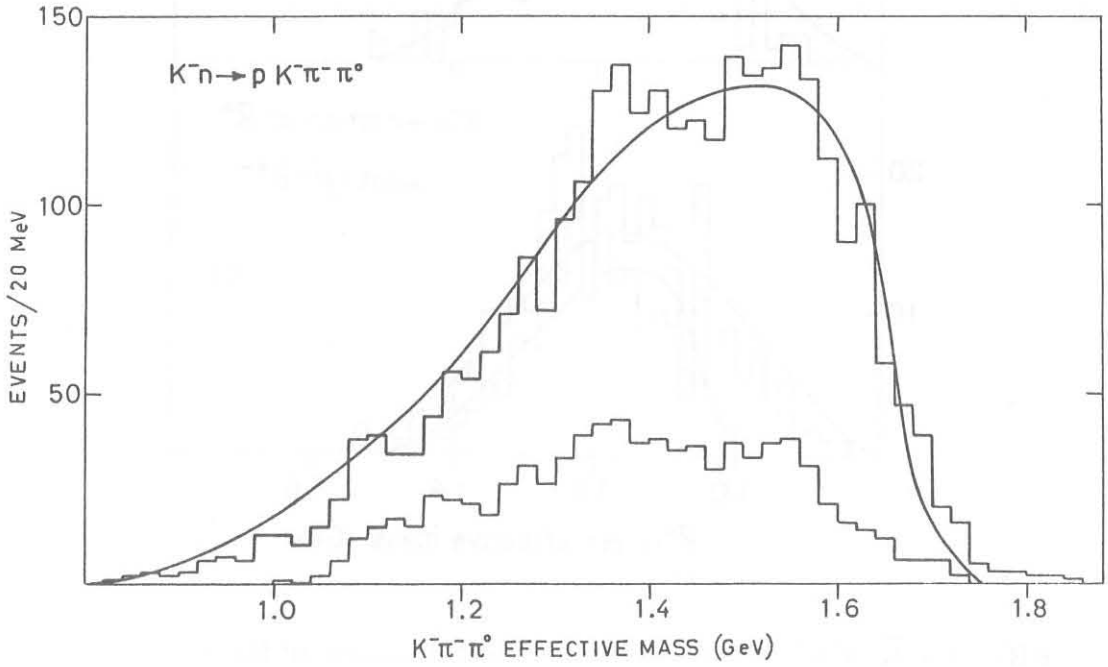

FIG. 3 - $K^-\pi^-\pi^0$ effective mass distribution in the $pK^-\pi^-\pi^0$ final state. The subset corresponds to $K^{*-}\pi^-$ events.

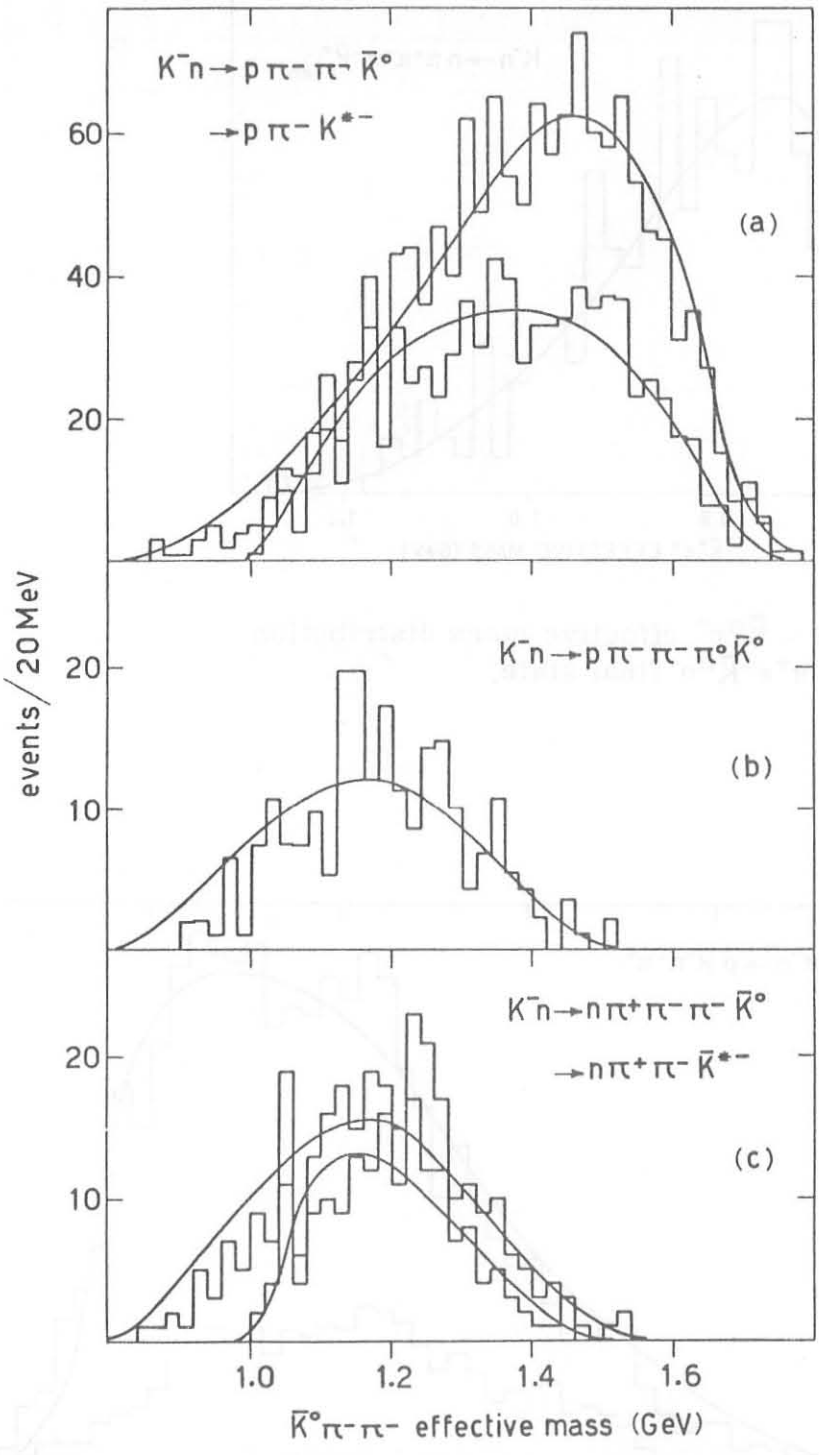

FIG. 4 - $\bar{K}^{o}\pi^{-}\pi^{-}$ effective mass distributions in the :
a) $p\pi^{-}\pi^{-}\bar{K}^{o}$ final state. The subset corresponds to $K^{*-}\pi^{-}$ events. The phase space for $K^{*-}\pi^{-}$ was computed assuming a fixed K^{*} mass.
b) $p\pi^{-}\pi^{-}\bar{K}^{o}\pi^{o}$ final state.
c) $\pi^{+}\pi^{-}\pi^{-}\bar{K}^{o}n$ final state. The subset corresponds to $K^{*-}\pi^{-}$ events.

3.2. - $(\bar{K}\pi\pi)^{--}$ states.

Figure 3 shows the $K^-\pi^-\pi^o$ effective mass distribution for the $pK^-\pi^-\pi^o$ final state. The subset corresponds to the $K^{*-}(890)\pi^-$ selection. In both the $K^-\pi^-\pi^o$ and $K^{*-}\pi^-$ distributions there could be some structure at about 1360 and 1540 MeV, the latter being at the top of phase space. If these bumps were true, they should also appear in the $\bar{K}^o\pi^-\pi^-$ and even more pronunced in the $K^{*-}\pi^-$ plots of the $p\pi^-\pi^-\bar{K}^o$ final state, where instead no significant structures are observed at these masses (Fig. 4a).

Figure 4 shows also the $\bar{K}^o\pi^-\pi^-$ effective masses for the $p\bar{K}^o\pi^-\pi^-\pi^o$ and $n\bar{K}^o\pi^+\pi^-\pi^-$ final states. The events of these reactions come all from the topologies where the $\bar{K}^o$ decay is observed. Small fluctuations may exist in Figs. 4b,c at a mass value of about 1260 MeV; the small number of events and the fact that they do not correspond to any structure in Fig. 4a, means very probably that they are simply statistical fluctuations.

Finally Figure 5 shows the $K^-\pi^-$MM distribution for the ($pK^-\pi^-$MM) final state. No phase space curve can be easily drawn for this final state; the enhancement seen around 1660 MeV is most probably due to reflections from normal resonance production (K^{*o} for instance).

We conclude that we have no clear evidence for any structure; in particular we do not observe the reported $(K\pi\pi)_{3/2}(1170)$[2] and $(K\pi\pi)_{3/2}(1270)$[12].

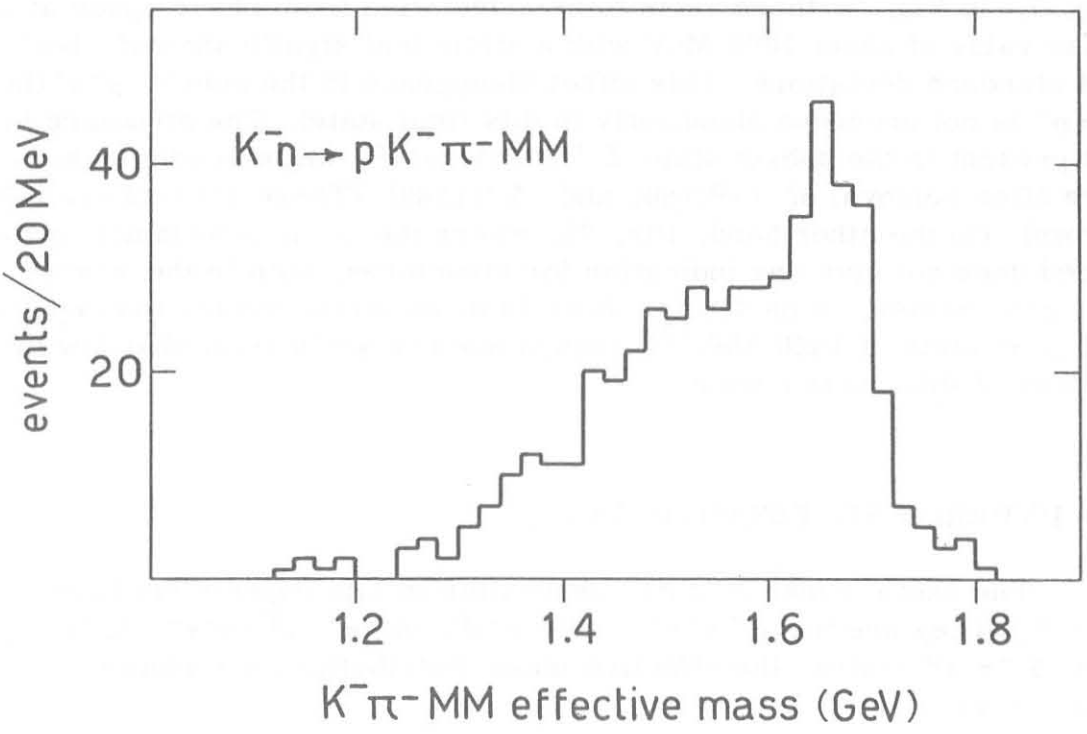

FIG. 5 - $K^-\pi^-$MM effective mass distribution in the $pK^-\pi^-$MM final state.

4. - NON-STRANGE MESONS. -

The exotic non-strange mesons accessible in this experiment have $I_z = -2$; they are the $\pi^-\pi^-$, $\pi^-\pi^-\pi^o$ and $\rho^-\pi^-$ states. The distributions concerning these states are shown in Figures 6 and 7.

The effective mass plots of Figs. 6a, b, c and 7c come from events belonging to the reactions discussed in the previous paragraph in connection with the $(\bar{K}\pi\pi)^{--}$ states. The other final states involve an hyperon (Λ^o, $\Sigma^{\pm}$ o) and many pions.

The events with a neutral hyperon belong to topologies where the decay products of the Λ^o are observed. Also the events with a charged Σ come from topologies where the charged decay product was observed.

On the average the various histograms for the $\pi^-\pi^-$ distributions follow the phase space predictions, with some fluctuations or possible structures in Figs. 6a, d, f (at the level of 2-4 standard deviations). These deviations do not correspond in mass when going from one graph to the other, suggesting that they are in reality fluctuations.

The subset in Fig. 6f corresponds to $\pi^-\pi^-$ produced backward in the c. m. system ($\cos\theta_{K^-,\pi^-\pi^-} < 0$), which corresponds to a reaction mechanism where a non exotic nucleon isobar may be exchanged. The subset looks remarkably free of fluctuations compared to the whole sample[16].

The $\pi^-\pi^-\pi^o$ and $\rho^-\pi^-$ effective mass distributions are shown in Fig. 7. In Fig. 7a there seem to be a deviation from phase space at a mass value of about 1000 MeV with a statistical significance of about 3-4 standard deviations. This effect disappears in the subset $\rho^-\pi^-$ (but the ρ^- is not produced abundantly in this final state). The structure is not present in the subset state $\Sigma^+(1383)\pi^-\pi^-\pi^o$, while seems to survive after removal of $\omega^o(780)$ and $\Sigma^-(1383)$ (These subsets are not shown). On the other hand, Fig. 7b, where the ρ^- is abundantly produced does not give any indication for structures, both in the $\pi^-\pi^-\pi^o$ and $\rho^-\pi^-$ states. In particular there is no confirmation for the reported $\rho^-\pi^-$ state at 1320 MeV[8], though our energy is somewhat low for a study of this mass region.

5. - HYPERON STATES WITH S = - 1.

The exotic hyperon states accessible in this experiment have $I_z = -2$. They are the $\Lambda^o\pi^-\pi^-$, $\Lambda^o\pi^-\pi^-\pi^o$, $nK^-\pi^-$, $n\bar{K}^o\pi^-\pi^-$, $\Sigma^-\pi^-$ and $\Sigma^-\pi^-\pi^o$ states; the effective mass distributions are shown in Figs. 8-12.

The events considered for the study of these hyperon exotic states are the same as those used for the study of the mesons, with the exception of the $\pi^+\Sigma^-\pi^-$ and $\pi^+\Sigma^-\pi^-\pi^o$ final states.

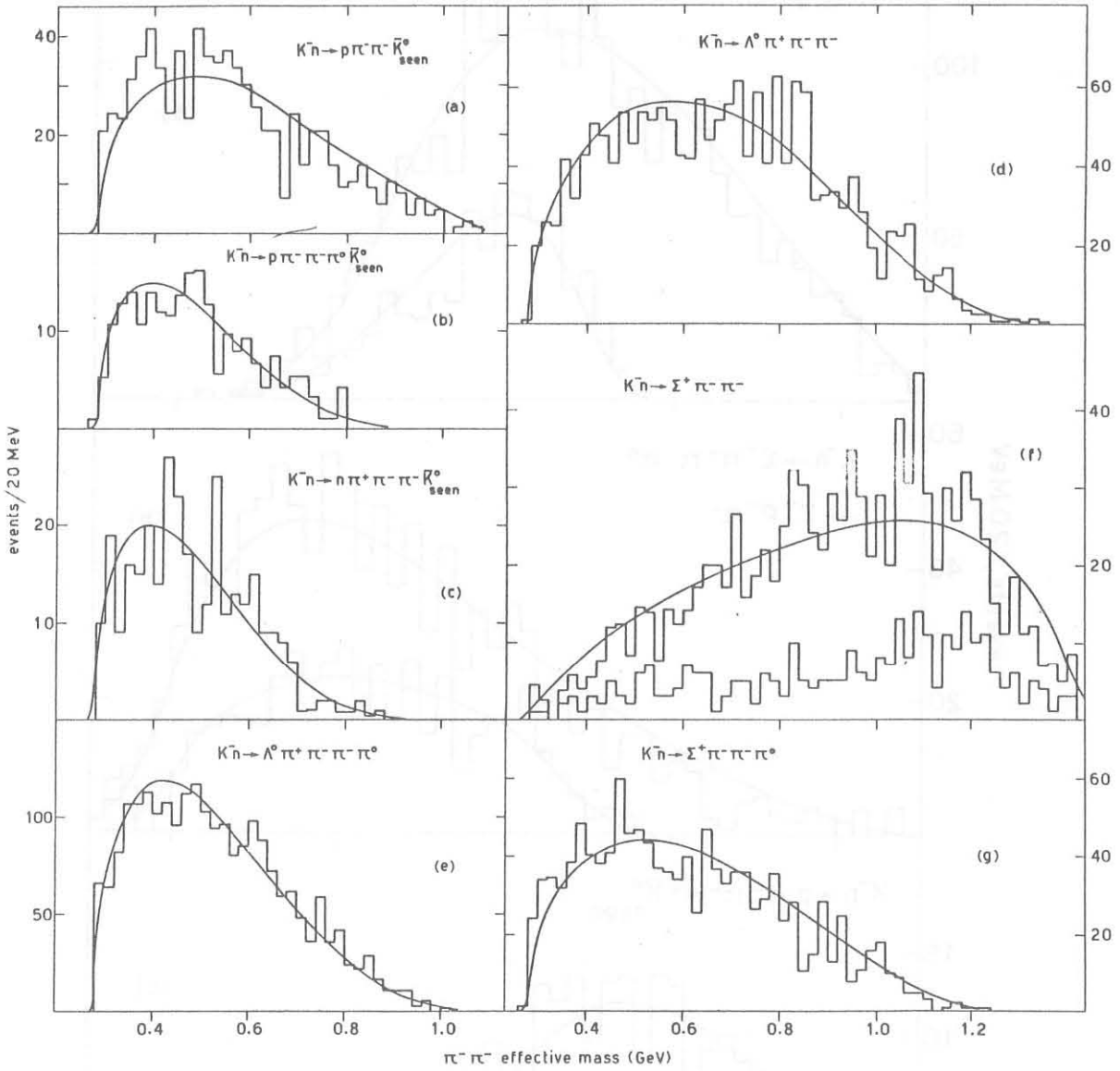

FIG. 6 - $\pi^-\pi^-$ effective mass distributions in the :
a) $p\pi^-\pi^-\overline{K}^o$ final state.
b) $p\pi^-\pi^-\overline{K}^o\pi^o$ final state.
c) $\pi^+\pi^-\pi^-\overline{K}^o n$ final state.
d) $\pi^+\pi^-\pi^-\Lambda^o$ final state.
e) $\pi^+\pi^-\pi^-\Lambda^o\pi^o$ final state.
f) $\Sigma^+\pi^-\pi^-$ final state. The subset refers to backward produced $\pi^-\pi^-$.
g) $\Sigma^+\pi^-\pi^-\pi^o$ final state.

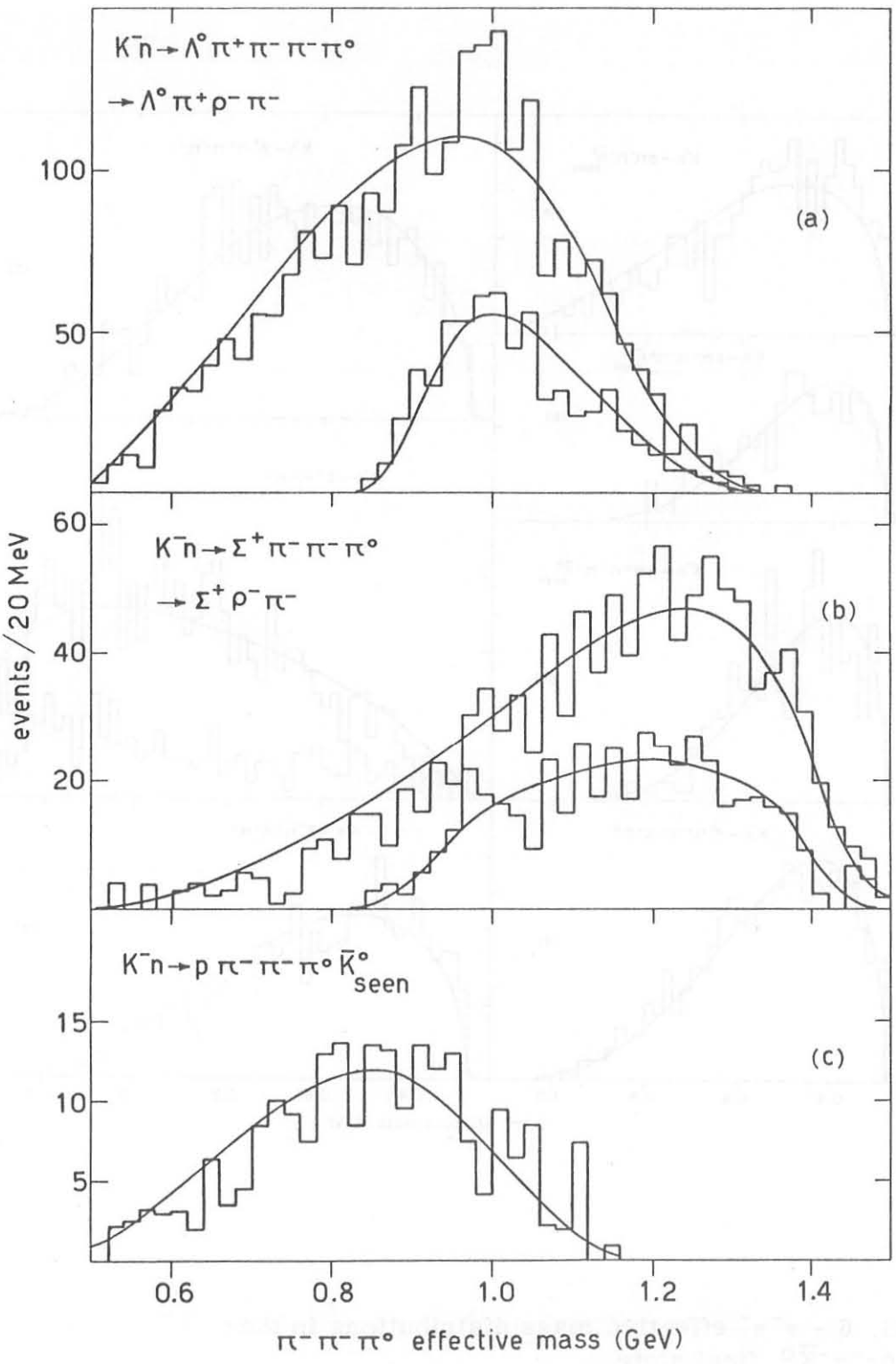

FIG. 7 - $\pi^-\pi^-\pi^o$ effective mass distributions in $\pi^+\pi^-\pi^-\Lambda^o\pi^o$, $\Sigma^+\pi^-\pi^-\pi^o$ and $p\pi^-\pi^-\bar{K}^o\pi^o$ final states. Shaded events correspond to $\rho^-\pi^-$; the phase space for $\rho^-\pi^-$ was computed assuming a fixed ρ mass (765 MeV).

Figure 8 shows the $\Lambda^o\pi^-\pi^-$ effective mass distributions in the two final states $\Lambda^o\pi^+\pi^-\pi^-$ and $\Lambda^o\pi^+\pi^-\pi^-\pi^o$ respectively.

In Figure 9 the small structure at the top of phase space (2360 MeV) has a statistical significance of about 3 standard deviations. Because of its location, its real significance is smaller.

Figure 10 shows the $nK^-\pi^-$ effective mass in the $nK^-\pi^+\pi^-$ final state and the $n\bar{K}^o\pi^-\pi^-$ mass in the $n\bar{K}^o\pi^+\pi^-\pi^-$ state. Similarly no significant structures are present in the histogram of the missing mass to the π^+ from the $K^-\pi^+\pi^-$ + neutrals final state (not shown in this report).

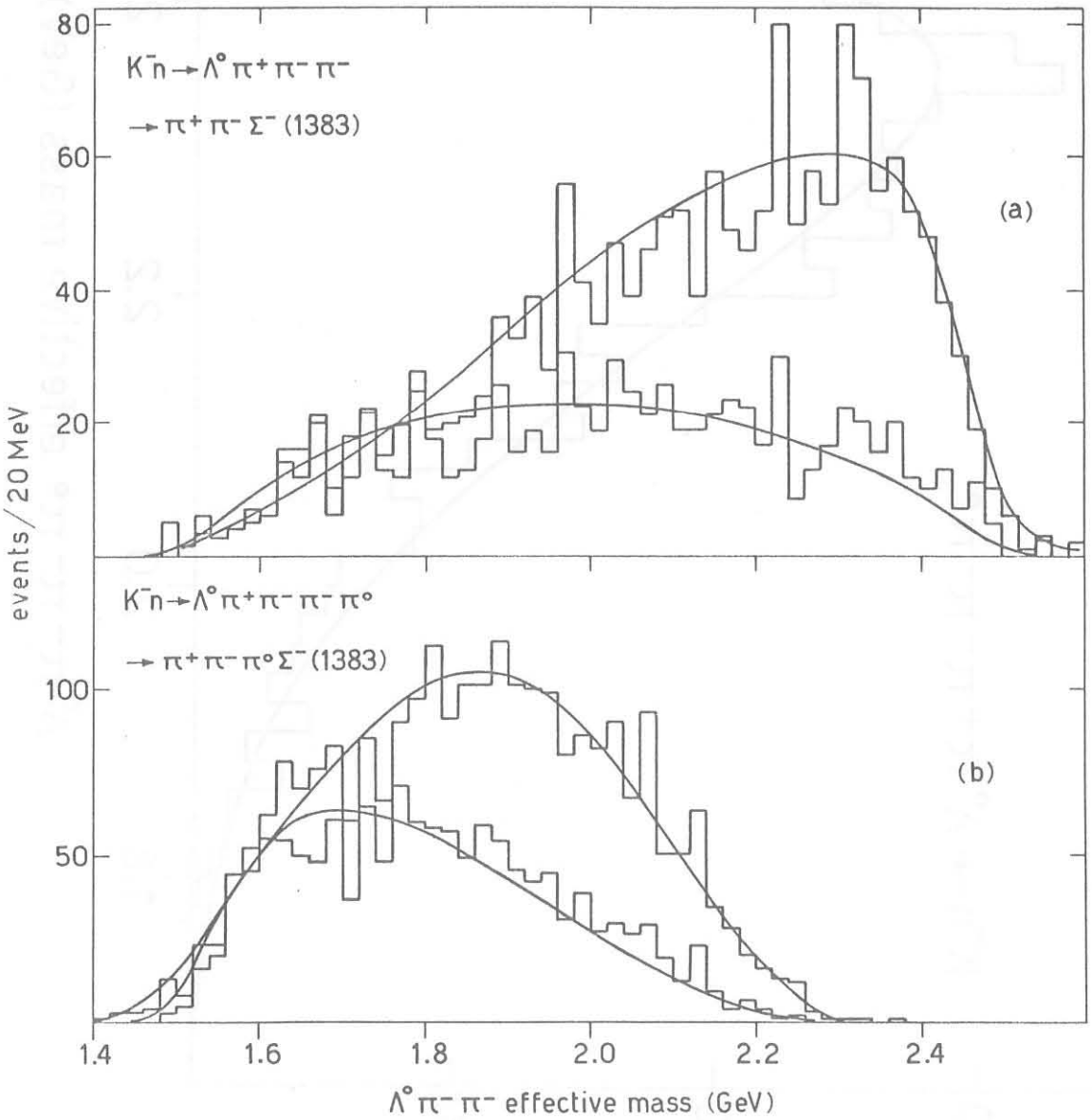

FIG. 8 - $\Lambda^o\pi^-\pi^-$ effective mass distributions in the :

a) $\pi^+\pi^-\pi^-\Lambda^o$ final state. The $\Sigma^-(1383)\pi^-$ events are shown in the subset.

b) $\pi^+\pi^-\pi^-\Lambda^o\pi^o$ final state. The subset corresponds to $\Sigma^-(1383)\pi^-$.

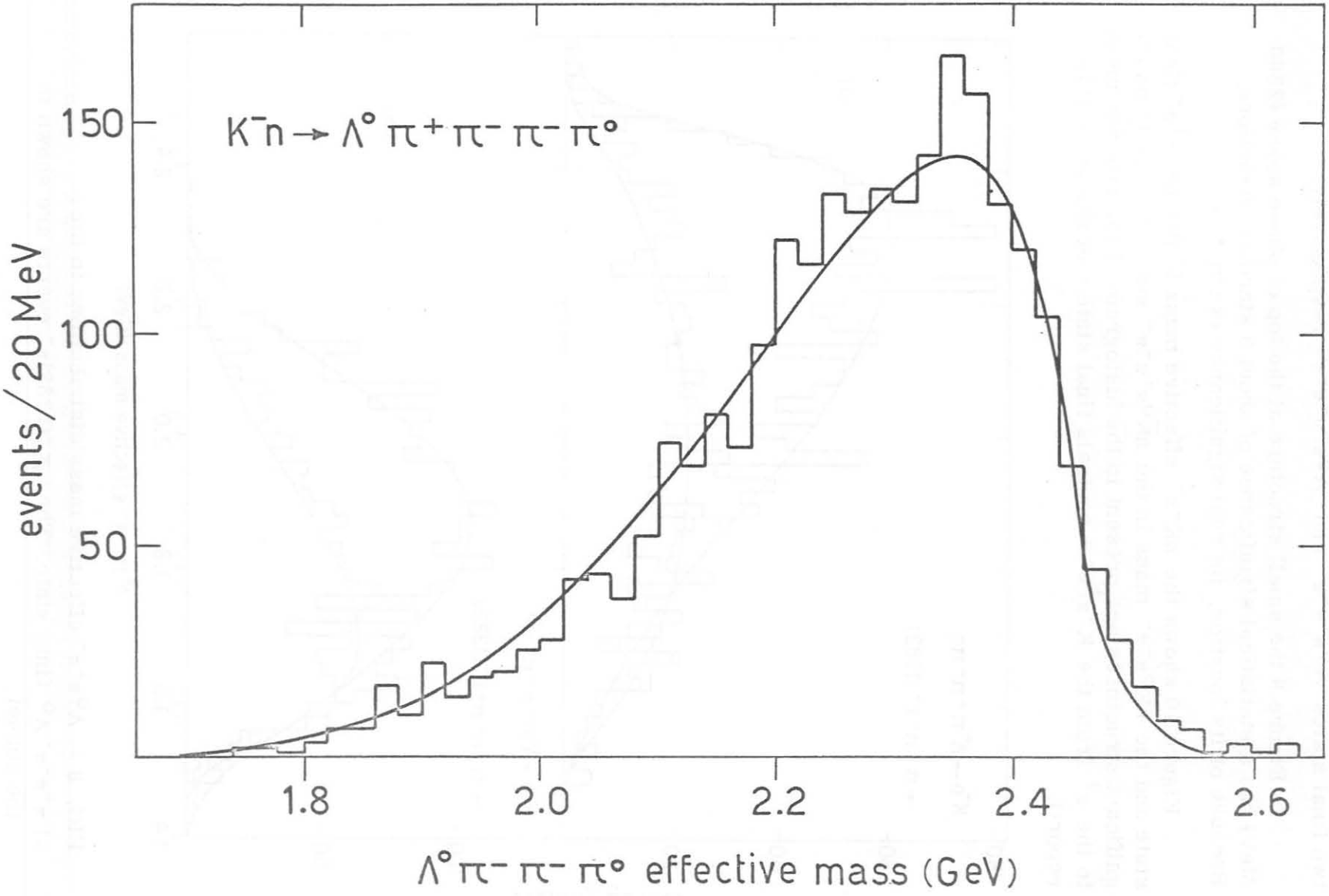

FIG. 9 - $\Lambda^\circ\pi^-\pi^-\pi^\circ$ effective mass distribution in the $\pi^+\pi^-\pi^-\Lambda^\circ\pi^\circ$ final state.

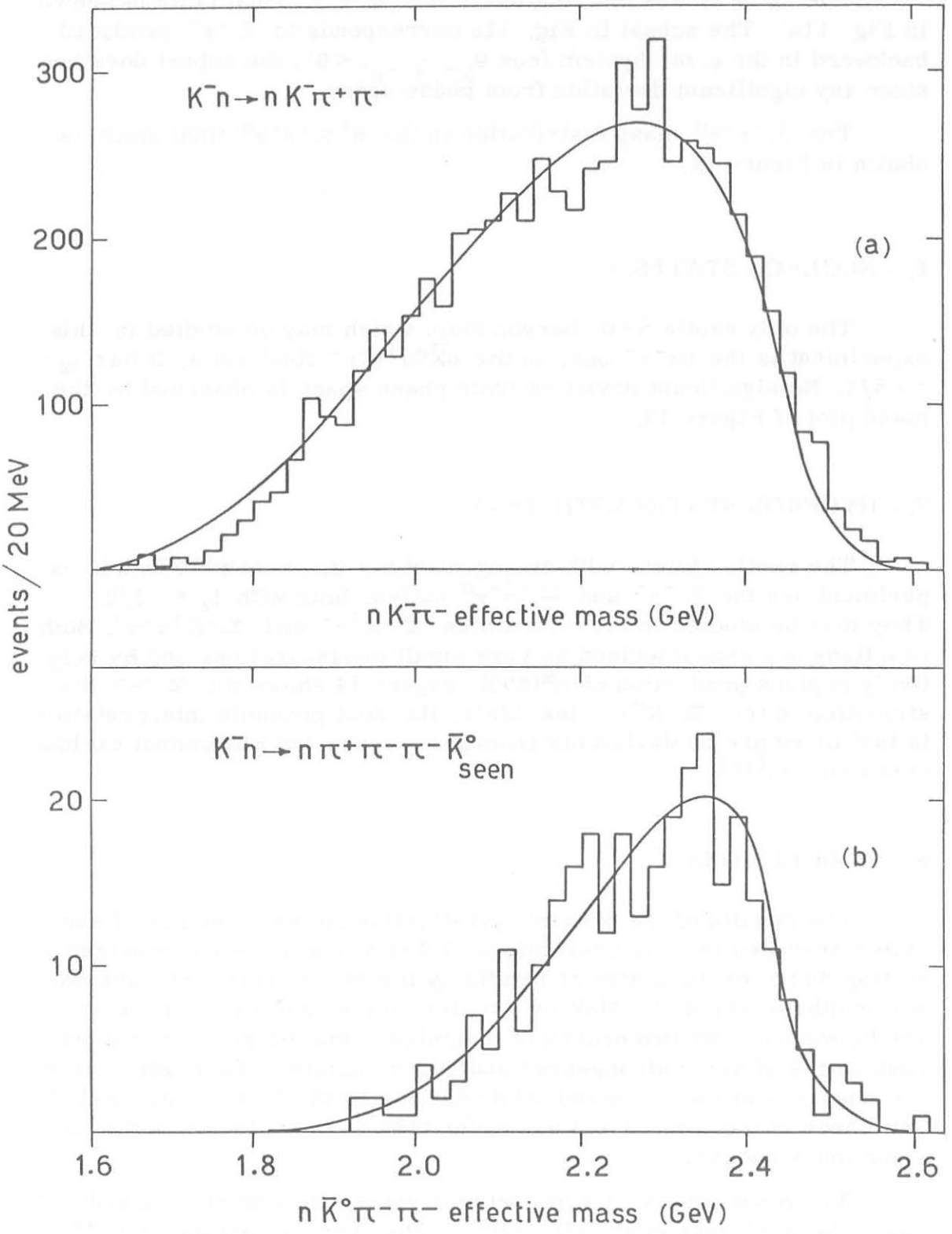

FIG. 10 -
a) $nK^-\pi^-$ effective mass distribution in the $\pi^+K^-\pi^-n$ final state;
b) $n\bar{K}^0\pi^-\pi^-$ effective mass distribution in the $\pi^+\pi^-\pi^-\bar{K}^0n$ final state.

The $\Sigma^-\pi^-$ mass distribution in the $\Sigma^-\pi^+\pi^-$ final state is shown in Fig. 11a. The subset in Fig. 11a corresponds to $\Sigma^-\pi^-$ produced backward in the c. m. system ($\cos\theta_{K^-,\Sigma^-\pi^-} < 0$); the subset does not show any significant deviation from phase space.

The $\Sigma^-\pi^-\pi^o$ mass distribution in the $\pi^+\Sigma^-\pi^-\pi^o$ final state is shown in Figure 12.

6. - NUCLEON STATES. -

The only exotic S = 0, baryon state which may be studied in this experiment is the $n\pi^-\pi^-$ one, in the $n\bar{K}^o\pi^+\pi^-\pi^-$ final state. It has $I_z = -5/2$. No significant deviation from phase space is observed in the mass plot of Figure 13.

7. - HYPERON STATES WITH S = - 2.

The exotic states, with strangeness S = -2, accessible in this experiment are the $\Xi^-\pi^-$ and $\Xi^-\pi^-\pi^o$ states, both with $I_z = -3/2$. They may be studied in the final states $\Xi^-K^+\pi^-$ and $\Xi^-K^+\pi^-\pi^o$. Both reactions are characterized by very small cross-sections and by relatively copious production of $K^*(890)$. Figure 14 shows the $\Xi^-\pi^-$ distribution in the $\Xi^-K^+\pi^-$ final state. Its most probable interpretation is that there are no deviations from phase space, but one cannot exclude small effects[19].

8. - CONCLUSIONS. -

The results of the present investigation on the existence of exotic states produced in K^-n interactions at 3 GeV/c may be summarized by stating that if exotic states of relatively low mass exist, and have normal widths of about 100 MeV or smaller, their production cross-sections are between one or two orders of magnitude smaller than for normal resonances of same strangeness and baryon number. Some structures are observed at the 2-4 standard deviations level. Their statistical significance is too limited and moreover they do not coincide in the various mass spectra.

We do not observe the reported $(K\pi\pi)_{3/2}$ mesons at 1170 and 1270 MeV, the $\rho^-\pi^-$ meson at 1320 MeV and the $(n\pi\pi)_{5/2}$ baryon at 1670 MeV.

We would like to acknowledge the co-operation of the other members of the SABRE collaboration and of the crew of the 81 cm bubble chamber. We thank our scanners and measurers for their untiring efforts.

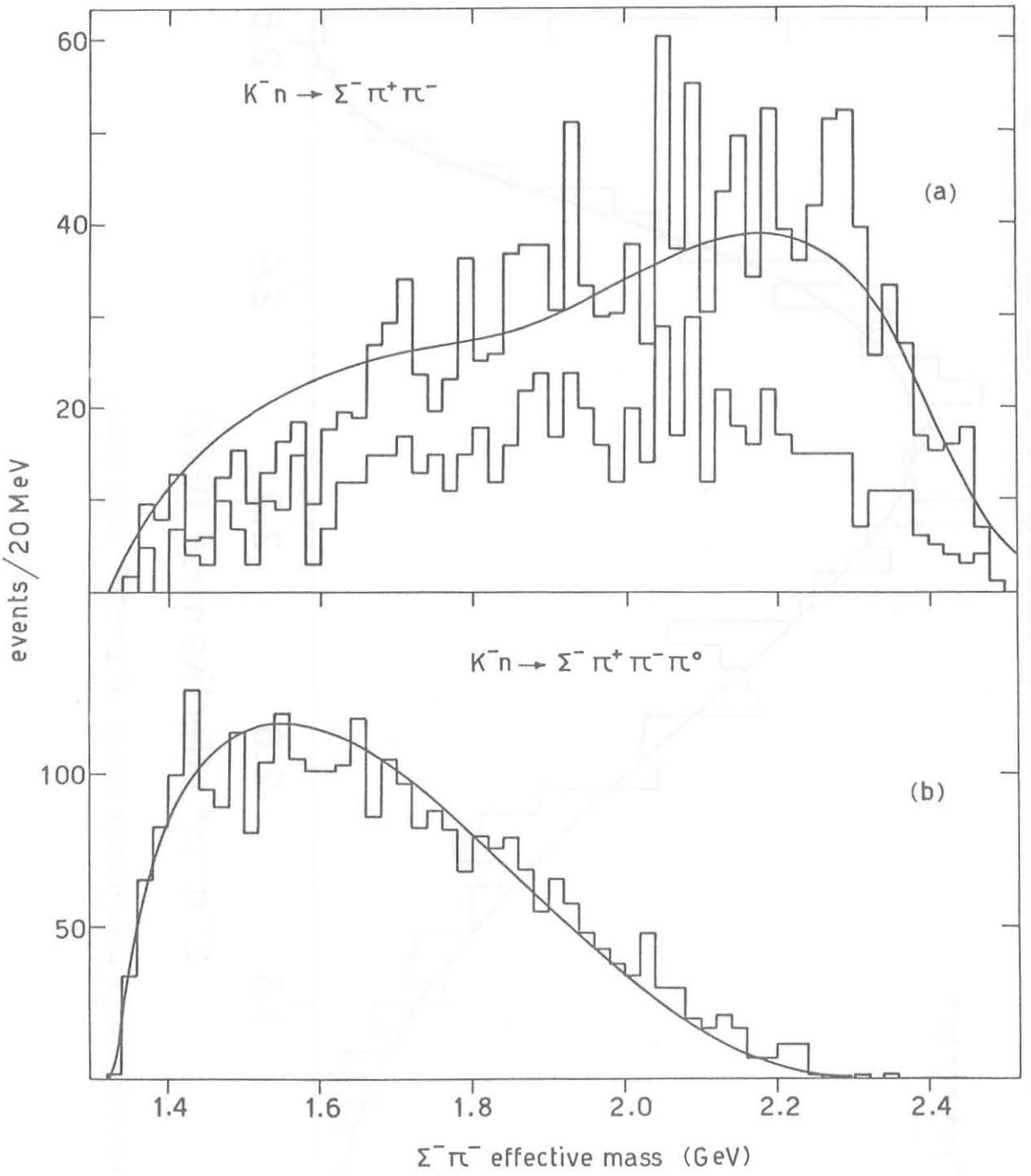

FIG. 11 - $\Sigma^- \pi^-$ effective mass distribution in the :

a) $\pi^+ \Sigma^- \pi^-$ final state. The subset corresponds to backward produced $\Sigma^- \pi^-$;

b) $\pi^+ \Sigma^- \pi^- \pi^o$ final state.

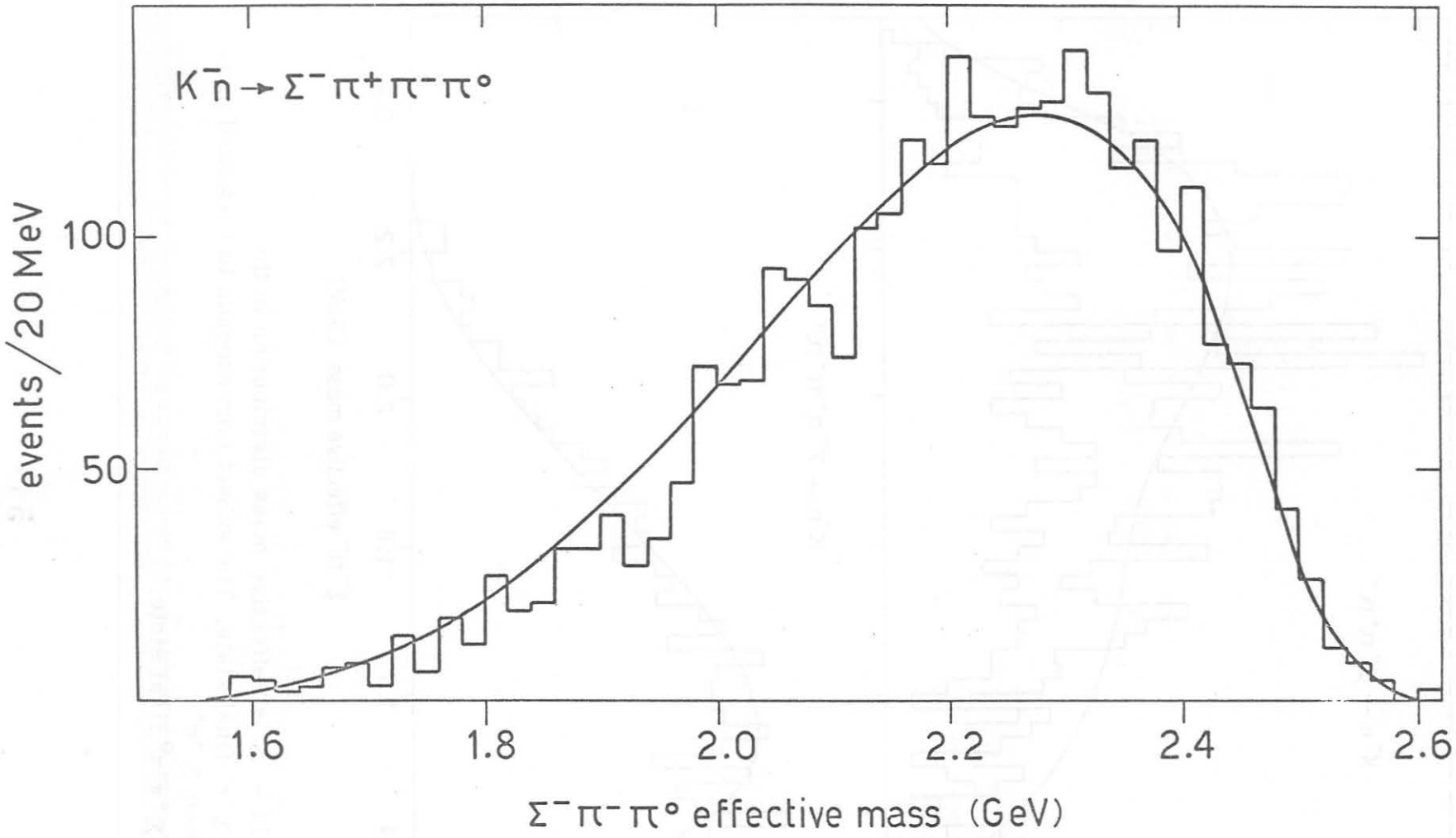

FIG. 12 - $\Sigma^-\pi^-\pi^o$ effective mass distribution in the $\pi^+\Sigma^-\pi^-\pi^o$ final state.

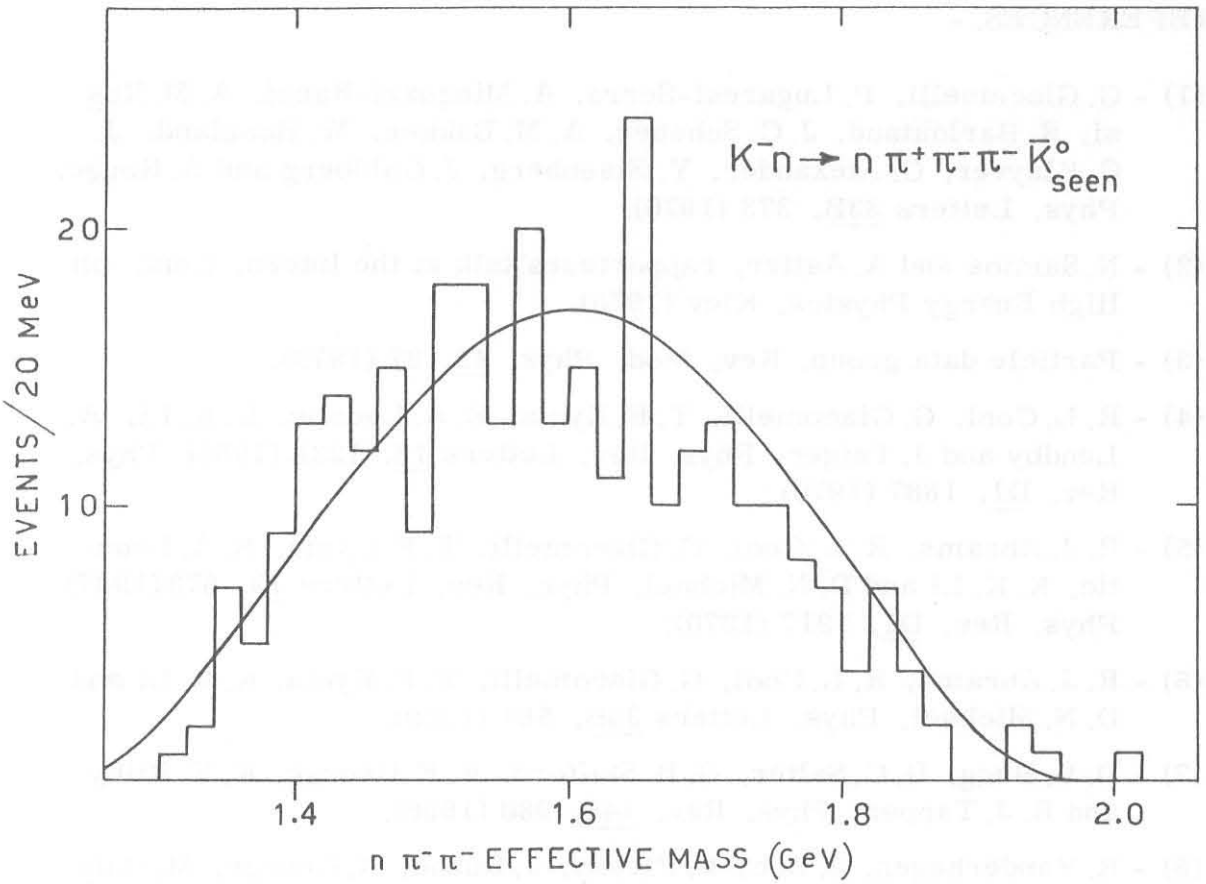

FIG. 13 - $n\pi^-\pi^-$ effective mass distribution in the $\pi^+\pi^-\pi^-\bar{K}^0n$ final state.

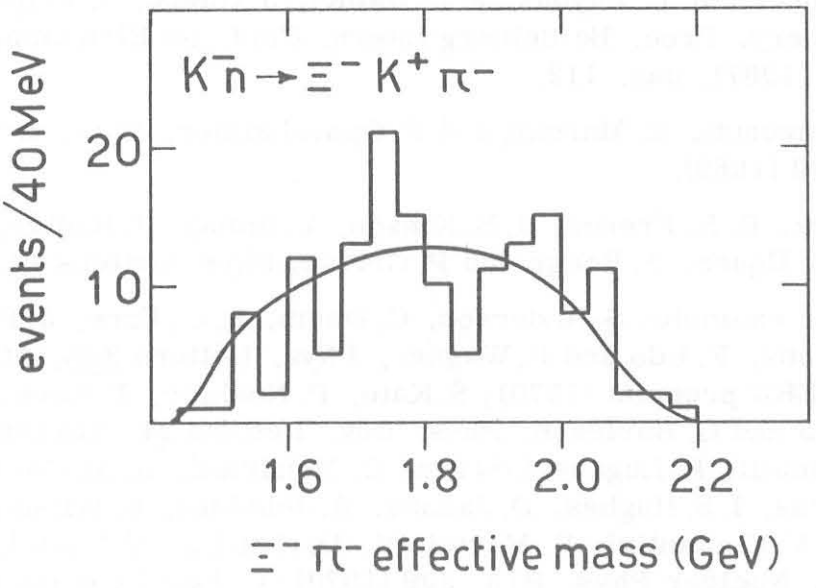

FIG. 14 - $\Xi^-\pi^-$ distribution in the $K^+\Xi^-\pi^-$ final state.

REFERENCES. -

(1) - G. Giacomelli, P. Lugaresi-Serra, A. Minguzzi-Ranzi, A. M. Rossi, R. Barloutaud, J. C. Scheuer, A. M. Bakker, W. Hoogland, J. C. Kluyver, G. Alexander, Y. Eisenberg, J. Goldberg and A. Rouge, Phys. Letters 33B, 373 (1970).

(2) - N. Samios and A. Astier, rapporteurs talk at the Intern. Conf. on High Energy Physics, Kiev (1970).

(3) - Particle data group, Rev. Mod. Phys. 42, 87 (1970).

(4) - R. L. Cool, G. Giacomelli, T. F. Kycia, B. A. Leontic, K. K. Li, A. Lundby and J. Teiger, Phys. Rev. Letters 16, 1228 (1966); Phys. Rev. D1, 1887 (1970).

(5) - R. J. Abrams, R. L. Cool, G. Giacomelli, T. F. Kycia, B. A. Leontic, K. K. Li and D. N. Michael, Phys. Rev. Letters 19, 678 (1967); Phys. Rev. D1, 1917 (1970).

(6) - R. J. Abrams, R. L. Cool, G. Giacomelli, T. F. Kycia, K. K. Li and D. N. Michael, Phys. Letters 30B, 564 (1969).

(7) - D. V. Bugg, D. C. Salter, G. H. Stafford, R. F. George, K. F. Riley and R. J. Tapper, Phys. Rev. 146, 980 (1966).

(8) - R. Vanderhagen, J. Huc, P. Fleury, J. Duboc, R. George, M. Goldberg, B. Makovski, N. Armenise, B. Ghidini, V. Picciarelli, A. Romano, A. Forino, R. Gessaroli, G. Quareni and A. Quareni-Vignudelli, Phys. Letters 24B, 493 (1967).

(9) - W. M. Katz, T. Ferbel, P. F. Slattery and H. Yuta, Phys. Letters 31B, 329 (1970).

(10) - M. Banner, M. L. Fayoux, J. L. Hamel, J. Cheze, J. Teiger and J. Zsembery, Proc. Heidelberg Intern. Conf. on Elementary Particles (1967), pag. 112.

(11) - A. Benvenuti, E. Marquit and F. Oppenhaimer, Phys. Rev. Letters 22, 970 (1969).

(12) - R. Böck, B. R. French, J. B. Kinson, V. Simak, J. Badier, M. Bazin, B. Equer, A. Rouge and P. Griese, Phys. Letters 12, 65 (1964).

(13) - See for example: S. Anderson, C. Daum, F. C. Erne, J. P. Lagnaux, J. C. Sens, F. Udo and F. Wagner, Phys. Letters 30B, 56 (1969) and CERN preprint (1970); S. Kato, P. Koehler, T. Novey, A. Yokosawa and G. Burleson, Phys. Rev. Letters 24, 615 (1970); G. Giacomelli, P. Lugaresi-Serra, G. Mandrioli, A. M. Rossi, F. Griffiths, I. S. Hughes, D. Jacobs, R. Jennings, B. Wilson, G. Ciapetti, V. Costantini, R. Martelotti, D. Zanello, E. Castelli and M. Sessa, Nuclear Phys. B18, 309 (1970); C. Lovelace and F. Wagner, CERN-TH 1251 (1970).

(14) - V. Barger, Rev. Mod. Phys. 40, 129 (1968).

(15) - P. M. Dauber, P. Hoch, R. J. Manning, D. M. Siegel, M. A. Abolins and G. A. Smith, Phys. Letters 29B, 609 (1969).

(16) - M. Jacob and J. Weyers, CERN-TH 1169 (1970).

(17) - D. Merril, R. Barloutaud, D. N. Hoa, J. C. Scheuer, A. Verglas, A. M. Bakker, A. J. De Groot, W. Hoogland, J. C. Klyver, A. G. Tenner, S. A. De Wit, S. Focardi, G. Giacomelli, A. Minguzzi-Ranzi, L. Monari, A. M. Rossi, P. Serra, B. Haber, A. Shapira, G. Alexander, Y. Eisenberg, E. Hirsch, G. Yekutieli, U. Karshon, J. Goldberg, E. Huffer, M. Laloum, G. Lamidey and A. Rougè, Nuclear Phys. B18, 403 (1970).

(18) - A. M. Bakker, W. Hoogland, J. C. Kluyver, G. Giacomelli, P. Lugaresi-Serra, A. M. Rossi, D. Merrill, J. C. Scheuer, G. Lamidey, A. Rougè, A. Shapira and U. Karshon, Nuclear Phys. B24, 211 (1970).

(19) - D. J. Crennel, U. Karshon, K. W. Lai, J. S. O'Neall, J. M. Scarr and T. G. Schumann, Phys. Rev. D1, 847 (1970).